Estimation of Curvature Based Shape Properties of Surfaces in 3D Grey-Value Images

Bernd Rieger, Lucas J. van Vliet, and Piet W. Verbeek

Pattern Recognition Group,
Department of Applied Physics, Delft University of Technology,
Lorentzweg 1, 2628 CJ, Delft, The Netherlands
{bernd,lucas,piet}@ph.tn.tudelft.nl

Abstract. Surfaces can be described locally and classified by their curvature values at every point. In this paper we investigate a grey-level based curvature estimator in combination with a sampling-error free integration technique of the curvature image. We compute shape descriptors as the bending energy and a global topological invariant, the Euler characterization. The integration of curvature values over the surface area is done by grey-volume integration. Our curvature estimator works on the orientation field of the surface, which does not require a segmentation of the surface. The estimated orientation fields has discontinuities mod π. It is mapped via the Knutsson mapping to a continuous representation in which the curvatures are computed.

1 Introduction

Curvatures of surfaces are the key to compute shape descriptors and to classify different classes of surfaces. We use an earlier presented method [6] to estimate principal curvatures of surfaces which are embedded in the image by a grey-level difference with respect to their surroundings. Our method works directly on the grey-value information of the image, neither a segmentation is needed to detect the curve nor a parametric fit is done at any time during the analysis.

Isophote curvature can successfully be applied to edges in 3D grey-value images [8], but it fails when applied to planar structures and shells (hollow objects) [9]. To overcome the problems associated with isophote curvature we transform the grey-value image into an orientation map (normal vector field up to sign) from which the curvatures can be derived after solving the discontinuity problem. We solve this problem by mapping the orientation field via the Knutsson mapping [4,6].

In order to build shape descriptors for objects based on these curvatures we must be able to integrate the curvatures over the whole object surface. We use a sampling error free surface area estimator based on the grey-volume of an object [8]. If the object is only defined by a shell/contour instead by a solid shape the shells must be filled to solid objects and then this volume is transformed to a volume proportional to the surface of the object [7]. With this techniques at hand we can now estimate the Euler characteristic the and bending energy. In images

J. Bigun and T. Gustavsson (Eds.): SCIA 2003, LNCS 2749, pp. 262–267, 2003.

that contain texture in the form of planar structures bending energy remains a useful characteristic (local deformation energy) and can be computed at every location with sub-pixel precision. We will apply it in section 5 to paper fibers, which are hollow cylinders (penne pasta) . A sphere minimizes bending energy for a given surface area. Therefore it can be seen as the roughness of a surface and can be used to characterize biological objects [3].

2 Mathematics

First we sketch the mathematics needed to compute curvatures on 2D surfaces that is relevant for our goal. The curvature κ at a point p in a tangent direction T on the surface is defined as the magnitude of the change of the surface normal N

$$\kappa_T(p) = \|\nabla_T N\| \,. \tag{1}$$

There exist two mutual orthogonal tangent direction T_1, T_2, for which the curvature is extremal. They are called principal directions, which associated curvatures κ_1, κ_2. Two measures of the curvature in point p are the Gaussian curvature $K := \det b = \kappa_1\kappa_2$ and the mean curvature $H := \frac{1}{2}\mathrm{tr}\, b = \frac{\kappa_1+\kappa_2}{2}$. From Gauss Theorema Egregium[2] we know that the Gaussian curvature is an isometry invariant, i.e. if a surface is bent without stretching K remains the same. In table 1 the shape of a surface is connected to the curvatures. A shape descriptor that

Table 1. Curvature and surface properties

H \ K	> 0	0	< 0
> 0	Peak	Ridge	Saddle ridge
0	-	Flat	Minimal surface
< 0	Pit	Valley	Saddle valley

κ_1 \ κ_2	> 0	0	< 0
> 0	Peak	Ridge	Saddle
0	Ridge	Flat	Valley
< 0	Saddle	Valley	Pit

can relate the shape of a 2D surface to its principal curvatures if $\kappa_1, \kappa_2 \neq 0$ by only one measure is the shape index $s = \frac{2}{\pi}\arctan\frac{\kappa_2+\kappa_1}{\kappa_2-\kappa_1} \in [-1, 1], \kappa_2 \geq \kappa_1$ [5]. Two shape properties can be expressed in terms of curvatures: the Euler characteristic and the bending energy. The Poincaré-Hopf index theorem states, that the integrated Gaussian curvature over a closed surface is an integer, the Euler characteristic χ

$$\int \kappa_1\kappa_2 \, dA = 2\pi\chi \,. \tag{2}$$

It describes the topology of the surface, and is in general the alternating sum of Betti numbers, which reads in 3D for polygons $\chi = n_{\text{vertices}} - n_{\text{edges}} + n_{\text{faces}}$.

The bending energy for a infinitesimal thin plate using elasticity theory is

$$\mathrm{BE}_{3D} = \int \kappa_1^2 + \kappa_2^2 \, dA \,, \tag{3}$$

neglecting material constants. For closed surfaces/shells the deformation properties are fundamentally different from plates. Stretching is here a first order effect and thus important even for small deflections. Nevertheless we can think of a surface as composed of a set of small rectangular patches, which can be bend without stretching, making it a well-defined shape descriptor in images.

3 Curvature of Surfaces in Grey-Level Images

The principal and normal direction can be found using an eigen analysis of the gradient structure tensor $\overline{G} := \overline{\nabla I \nabla I^t} = \sum \lambda_i v_i$, where I is a grey-value image and the overhead bar stands for averaging the elements over a local neighborhood σ_T. The eigenvectors $\{v_i\}$ only contain orientation information (discontinuity mod π) but they are mapped via the Knutsson mapping $M(v) := vv^t/\|v\|$ to a closed orientation representation [4,6]. Summarizing we have:

$$v_1 \leftrightarrow N,\ v_{2,3} \leftrightarrow T_{1,2}\,, \tag{4}$$

and the curvatures are computed in extension to (1) as [6]

$$|\kappa_{1,2}| = \frac{1}{\sqrt{2}} \|\nabla_{v_{2,3}} M(v_1)\|\,. \tag{5}$$

4 Bending Energy, Euler Characteristic, and Surface Area

We test our algorithm on bandlimited grey-value test images containing shells of constant thickness of spheres and ellipsoids. Isophote curvature estimation $\frac{I_{TT}}{\|\nabla I\|}$ applied to these images will fail as the gradient vanishes on ridges and valleys.

The performance of the algorithm is investigated for ellipsoids as a function of scale and deformation. In all experiments the results of the true, the noise free and two noise levels (20, 40dB) are plotted. The noise runs are averaged over 20 realization and the noise free over 20 sub-pixel shifts. The Euler characteristic is $\chi = 2$ for any closed surface without holes. The results of our computations are shown in figure 1a) for a scaled ellipsoid and in figure 1b) for a deformed one. The deformation of an ellipsoid is done by slowly deforming a sphere ($r = 12$) into a elongated cigar like object ($a = c = 12, b = 38$). The scaled ellipsoid is blown up from $a = c = 12, b = 18$ to $a = c = 36, b = 54$ with constant $b/a = 1.5$.

The area estimation $\int dA \leftrightarrow \sum \|\nabla I\|$ [8] is critical to all other estimations. For the noise free case the estimation is excellent, for small curvatures the estimation error is smaller than 0.5%. The bending energy and the Euler characteristic are scale invariant properties. In figure 1a) we see that the run of the curve for the noise free and 40dB indeed approaches a constant value. For 20dB the curvature estimation for larger ellipsoids seems to be influenced by the noise in a scale variant manner, as the area estimation remains fine. As higher curvatures are more biased we expect the estimation to perform better for larger ellipsoids. The

quality of the estimation of the bending energy and the Euler characterization, however, decrease with increasing elongation. The curvature increases in some areas during deformation such that the bending energy increases.

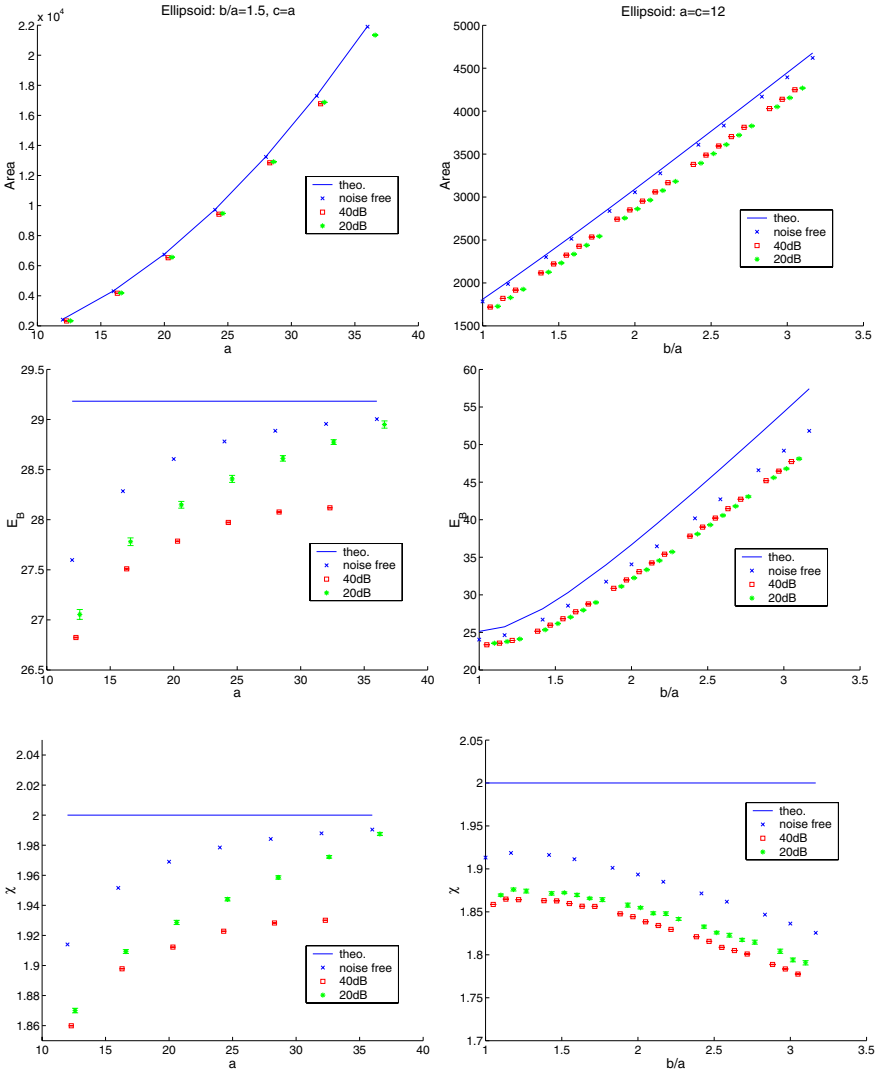

Fig. 1. Surface area, bending energy and Euler characterization estimation at different noise levels averaged over 20 runs for a) scaled ellipsoid, b) deformed ellipsoid, $\sigma_g = 1, \sigma_T = 2, \sigma_k = 1$

5 Application: Bending Energy of Paper Fibers

In figure 2a) we show part of a, pre-processed, SEM scan of duplex board paper, of which for example milk cartons are made of. The image size is $3072 \times 768 \times 102$ voxels with a voxel size of $0.7 \times 0.7 \times 5 \mu$m. The image was provided by StoraEnso Research, Sweden. We compute the curvature and bending energy via (5) and the isophote curvature, see figure 2b) and c). The bending energy is only displayed for regions where fiber is present. With our algorithm the deformed parts are directly highlighted as bright parts whereas the isophote curvature has difficulties dealing with the ridge-like cross-section of the image structure. The different paper fibers

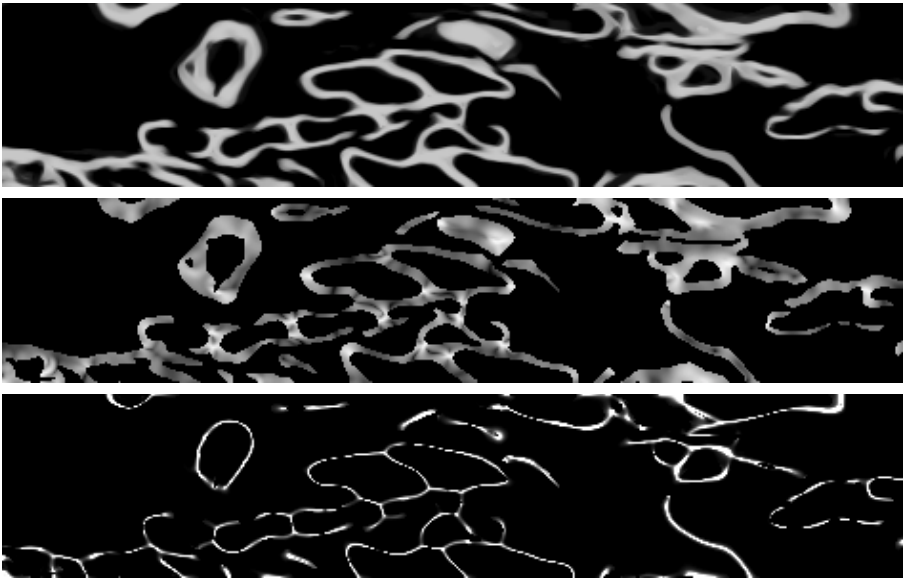

Fig. 2. A $33 \times 67 \mu$m region of a SEM paper scan at depth of 73μm a) adaptive filtered input, b) bending energy via (5), log stretch, $\sigma_g = 1, \sigma_T = 3$ c) bending energy via the isophote curvature, range [0,0.5], $\sigma = 3$

can be segmented[1] and then the bending energy can be integrated over each fiber. The deviation of their bending energy from a cylinder provides a measure for the deformation of the fiber. This contains more shape information than a pure fiber curl measure[1], where just the distance between start and end-point is compared to the middle line length.

6 Conclusion

We have demonstrated that our approach to curvature and (local) shape descriptors on surfaces based on the differential structure of images is working. It

avoids problems associated with classical approaches such as matched filtering, isophote curvature and polynomial fitting. Curvature based shape descriptors, the bending energy and Euler characterization χ, can be computed. The later as a function of scale is closely related to the morphological granulometry, which is a volume weighted distribution and χ only counts the number of objects visible at a certain scale. The estimation of these descriptors is consistent, robust and independent of the scale of the objects. It performs excellent for isotropic objects and small curvature ($\epsilon < 0.05\%$ for $\kappa < 0.03$), for highly asymmetric shapes and high curvatures the error stays small ($\epsilon < 5\%$ for $\kappa < 0.09$).

Acknowledgements. This work was partially supported by the Netherlands Organization for Scientific Research NWO, grant number 612-012-003. The paper fiber volume SEM scan has be kindly provided by O. Sävborg and O. Henningsson from StoraEnso Research, Falun, Sweden.

References

1. M. Aronsson. *On 3D Fibre Measurement of Digitized Paper*. PhD thesis, Swedish University of Agricultural Science, Uppsala, Sweden, 2002.
2. M.P. do Carmo. *Differential Geometry of Curves and Surfaces*. Prentice Hall, New Jersey, 1976.
3. J.S. Duncan, F.A. Lee, A.W.M. Smeulders, and B.L. Zaret. A bending energy model for measurement of cardiac shape deformaty. *IEEE Transactions on Medical Imaging*, 10(3):307–319, 1991.
4. H. Knutsson. Representing local structure using tensors. In *The 6th Scandinavian Conference in Image Analysis*, pages 244–251, Oulu, Finland, June 19-22 1989.
5. J.J. Koenderink and A.J. van Doorn. Surface shape and curvature scales. *Image and Vision Computing*, 10(8):557–565, 1992.
6. B. Rieger, F.J. Timmermans, L.J. van Vliet, and P.W. Verbeek. Curvature estimation of surfaces in 3d grey-value images. In C. Suen R. Kasturi, D. Laurendeau, editor, *ICPR'02, Proc. 16th Int. Conf. on Pattern Recognition*, volume 1. IEEE Computer Society, August 11–15 2002.
7. P.W. Verbeek and J. Dijk. The D-dimensional inverse vector-gradient operator and its application for scale free image enhancement. In *10th International Conference on Computer Analysis of Images and Patterns (Gronigen, The Netherlands)*, August 25-27 2003.
8. L.J. van Vliet and P.W. Verbeek. Curvature and bending energy in digitized 2d and 3d images. In *SCIA'93*, pages 1403–1410, Tromsø, Norway, 1993.
9. J. van de Weijer, L.J. van Vliet, P.W. Verbeek, and M. van Ginkel. Curvature estimation in oriented patterns using curvilinear models applied to gradient vector fields. *IEEE Transactions on Pattern Analysis and Machine Intelligence*, 23(9):1035 –1042, 2001.